machines

MDPI

Article

Properties of Cutting Tool Composite Material Diamond–(Fe–Ni–Cu–Sn) Reinforced with Nano-VN

Athanasios Mamalis [1], Vladimir Mechnik [2], Dmitrij Morozow [3,*], Boranbay Ratov [4], Vasyl Kolodnitskyi [2], Waldemar Samociuk [5,*] and Nikolai Bondarenko [2]

1 Project Center for Nanotechnology and Advanced Engineering, 9 Finikos Street, Kifissia, 14564 Athens, Greece; agmamalis@yahoo.com
2 V. Bakul Institute for Superhard Materials of the NAS of Ukraine, 04074 Kyiv, Ukraine; vlad.me4nik@ukr.net (V.M.); vasylkolod56@gmail.com (V.K.); bond@ism.kiev.ua (N.B.)
3 Faculty of Mechanical Engineering Kazimierz Pulaski, University of Technology and Humanities in Radom, Stasieckiego 54, 26-600 Radom, Poland
4 Institute of Geology, Oil and Mining, K. Satpayev Kazakh National Technical University, 050013 Almaty, Kazakhstan; ratov.bt@gmail.com
5 Faculty of Production Engineering, Lublin University of Life Sciences, Gleboka 28, 20-612 Lublin, Poland
* Correspondence: d.morozow@uthrad.pl (D.M.); waldemar.samociuk@up.lublin.pl (W.S.)

Abstract: The study is devoted to structure and mechanical properties of a diamond composite used for manufacturing of cutting tools applied in a wide range of technological fields. The sample tools were fabricated by cold-pressing technology followed by hot-pressing in vacuum of the 51Fe–32Cu–9Ni–8Sn matrix mixture with diamond bits, both in absence and presence of nano-VN additives. It was demonstrated that without VN addition, the diamond–matrix interface contained voids and discontinuities. Nanodispersed VN added to the matrix resulted in the formation of a more fine-grained structure consisting of solid solutions composed of iron, copper, nickel, vanadium and tin in different ratios and the formation of a tight diamond–matrix zone with no visible voids, discontinuities and other defects. Optimal concentrations of VN in the CDM matrix were found achieving the maximum values of nanohardness H = 7.8 GPa, elastic modulus E = 213 GPa, resistance to elastic deformation expressed by ratio H/E = 0.0366, plastic deformation resistance H^3/E^2 = 10.46 MPa, ultimate flexural strength R_{bm} = 1110 MPa, and compressive strength R_{cm} = 1410 MPa. As-prepared Fe–Cu–Ni–Sn–VN composites with enhanced physical and mechanical properties are suitable for cutting tools of increased durability and improved performance.

Keywords: cutting tools; composite; nanodispersed vanadium nitride; vacuum hot pressing; structure; elastic strain to failure; resistance to plastic deformation

check for updates

Citation: Mamalis, A.; Mechnik, V.; Morozow, D.; Ratov, B.; Kolodnitskyi, V.; Samociuk, W.; Bondarenko, N. Properties of Cutting Tool Composite Material Diamond–(Fe–Ni–Cu–Sn) Reinforced with Nano-VN. *Machines* **2022**, *10*, 410. https://doi.org/10.3390/machines10060410

Academic Editor: Raul D. S. G. Campilho

Received: 27 April 2022
Accepted: 20 May 2022
Published: 24 May 2022

1. Introduction

The latest technological evolution imposes new and strict requirements on the strength and durability of cutting tools, especially those working in harsh conditions under heavy loads [1]. In this context, the improvement of physical and mechanical properties of diamond composites used for the manufacturing of cutting tools applied in a wide range of technological fields, is of crucial importance. These materials are required to combine high physical, mechanical and performance characteristics, such as hardness, elastic modulus, fracture toughness, thermal conductivity, plasticity, high diamond retention capacity, friction coefficient, thermal and wear resistance [2–4]. It is well-established knowledge that the wear resistance of diamond composites depends on the elemental composition and properties of a matrix, either a metal or carbide one [5–7], the strength and shape of diamond grains [8,9], their concentration [10], as well as the abrasiveness and productivity of rock processing [11]. The wear mechanism of the diamond composite cutting tools during rock cutting has been studied in detail in [12]. Intentional changing of the composite structure and phase composition enables a significant effect on their physical-mechanical and

performance properties [13–18]. Alterations in the chemical composition yield structural components in their metal matrices providing significantly higher performance properties as compared to the original diamond composite [19,20].

Among materials for cutting-off wheels, wire saws and other tools used in stone processing and mining industries, diamond composites based on Fe–Cu–Ni–Sn matrices are preferred. As compared to the ones based on WC–Co alloy matrices, they exhibit high cutting qualities and are less prone to brittle fracturing [21,22], which allows for using them in cutting rock applications under varying strength and abrasiveness. In addition, diamond composites based on Fe–Cu–Ni–Sn matrices, exhibit advantages as follows:

- appearance of a liquid phase at a relatively low temperature during sintering in the Cu–Sn system, which contributes to preserving the strength of diamond bits;
- the ability of metal matrix components to undergo cold pressing, which makes it possible to form tools of different shapes and expand the limits of their applications;
- the low cost of metal matrix components;
- the absence of toxic cobalt, and ability to improve environmental conditions.

However, due to the increased operating loads and warranty periods of the above diamond composite tools, it is imperative to develop new ones and to constantly look for ways to improve the existing materials.

In the latter activity, it is important to consider typical disadvantages of the existing diamond composites, among others insufficient hardness of the matrix material and low values of H/E and H^3/E^2, which indicate the material elastic strain to failure [23] and resistance to plastic deformation [24], respectively. Other authors indicate inadequate ultimate flexural strength R_{bm}, and the appearance of graphite inclusions in the diamond–matrix transition zone due to graphitization of diamond bits during sintering [25–27]. These result in the failure of the cutting tools when the diamonds are torn out from the matrix.

Numerous studies aimed at improvement of the physical and mechanical properties of the diamond composites have been undertaken intensively over the past decade. These studies are driven by the study of composition and structural features, explained by the "composition–structure–dispersion–properties" relation for these materials [28–30]. The incorporation of small amounts of additives can promote the reduction of grain size, increase the stiffness and elastic modulus as well as the metal matrix wear resistance, and prevent the micro-crack formation in a matrix [31]. For instance, in [32] it was shown that mechanical properties and wear resistance of a diamond composite based on Fe-matrix improved after CeO_2 was added. In [33,34] it was demonstrated that the addition of CrB_2 micropowder in an amount of 2 wt.% to 51Fe–32Cu–9Ni–8Sn matrix provided decarburization in the diamond–matrix transition zone due to the formation of Cr_3C_2, Cr_7C_3, Fe_3C i $Cr_{1{\cdot}65}Fe_{0{\cdot}35}B_{0{\cdot}96}$ interlayers, which increased wear resistance of the diamond composite. In [35], it was demonstrated that an increase in CrB2 concentration in the 51Fe–32Cu–9Ni–8Sn-based composite content was accompanied by an increase in its stiffness and elastic modulus. At the same time, the friction coefficient and wear rate decreased when the CrB_2 content increased up to 2 wt.%. In the initial researches [36,37] it was proved that when vanadium nitride nanopowder (nano-VN) was added to 51Fe–32Cu–9Ni–8Sn composite, it exhibited significantly higher nanohardness H, elastic modulus E, and H/E values. The mechanism of the physical properties improvement of 51Fe–32Cu–9Ni–8Sn composite containing nano-VN admixture is conditioned by $\alpha \rightarrow \gamma \rightarrow \alpha$ transformations under the dissolution of VN in α-Fe and its subsequent cooling that promotes concurrent refinement of its structure [38]. It is worth noting that transition to the nanometer-size state increases the specific surface area of a diamond composite, while its mass remains unchanged. Moreover, its volume decreases due to better compaction and reduction of porosity, which results in the improvement of physical and mechanical properties.

This research is dedicated to the determination of the optimum percentage of nano-VN in a 51Fe–32Cu–9Ni–8Sn matrix and its effect on the structure. diamond grain concentration and mechanical (nanohardness H, elastic modulus E, material elastic deformation resistance H/E, material plastic deformation resistance H^3/E^2, fracture toughness K_{Ic}, compressive

strength R_{cm} and flexural strength R_{bm}) properties formed by cold-pressing and subsequent vacuum hot-pressing.

2. Materials and Methods

2.1. Sample Preparation

For sintering samples of diamond reinforced metal matrix composite, the following powders were used: iron PZ1M2, copper PMS-1, nickel PNE, and tin PO-1, all produced by Powder Metallurgy Plant SE (Zaporizhzhia, Ukraine), and vanadium nitride CASRN 24646-85-3, delivered by ONYXMET (Olsztyn, Poland). The average particle size of Fe powder was 25 µm ± 10 µm, that of Cu powder 20 µm ± 9 µm, Ni powder 15 µm ± 8 µm, Sn powder 15 µm ± 8 µm, and VN powder 0.5µm ± 0.1 µm. Powders in relevant proportions were mixed together in an offset mixer for 8 h. The specific power consumption of the mixer was 8 W/h. The content of initial mixtures for further sintering of the samples is presented in Table 1.

Table 1. Percentage of the components in the tested samples, wt.%.

Sample No.	Fe	Cu	Ni	Sn	VN
1	51	32	9	8	–
2	50.745	31.84	8.955	7.96	0.5
3	50.49	31.68	8.91	7.92	1
4	50.235	31.52	8.865	7.88	1.5
5	49.98	31.36	8.82	7.84	2
6	48.96	30.72	8.64	7.68	4
7	47.94	30.08	8.46	7.52	6
8	46.92	29.44	8.28	7.36	8
9	45.9	28.8	8.1	7.2	10

Using a hydraulic press, the prepared mixtures were pressed at room temperature in heat-resistant alloy moulds at a pressure of 500 MPa. As-prepared samples were then sintered in graphite forms in vacuum hot pressing device described in detail in [39]. The temperature range was from 20 °C up to 1000 °C, the pressure was 30 MPa, and sintering time was 5 min. Then, the sintered samples underwent grinding and thus the cylinders with diameter of 9.62 mm and thickness of 4.84 mm were achieved. These were used for examination of the matrix material properties.

To study the properties of the diamond composite, and especially diamond–matrix transition zone and fracture characteristics, samples of size 35 × 12 × 2 mm were prepared as follows. AC160T diamond powder of 400/315 granularity, made by Diaprom OOO, (Kiev, Ukraine), in the amount of 1.54 carats per 1 cm^3 was added to the powder mixtures, which corresponded to the relative concentration K = 35% in the mixtures specified in Table 1. Diamonds were mixed into the powders in an ethanol medium. After sintering, the samples destined for microstructural and mechanical studies, were polished using 1 µm particle diamond paste and colloidal solution with silicon oxide particles of 0.04 µm to obtain a mirror-like surface.

2.2. Microstructure and Micromechanical Characteristics

The study on morphology, microstructure, and surface elemental composition of the samples, was performed using Mira 3 LMU scanning electron microscope (SEM) made by Tescan (Brno, Czech Republic) with a spatial resolution of 1 nm and acceleration potential of 30 kV. The crystal structure and phase composition of sintered samples were examined by the X-ray diffractometry (XRD) using DRON-4 diffractometer produced by Bourevestnik (Saint-Petersburg, Russia) in Cu$K\alpha$ radiation with λ_{Cu} = 0.1542 nm.

Hardness H and elastic modulus E of sintered samples were determined using a triangular Berkovich type indenter according to the recognized Oliver–Pharr method [40]. For that purpose, a nano-hardness tester Nano Indentor G200 (made by Agilent Technologies,

Santa Clara, CA, USA) was used. The depth of nanoindentation was 500 nm. Tests were performed on the samples with different content of VN. At least 10 tests were performed for each sample, then the results were averaged. During testing the load dependence of indenter, immersion was recorded. The physical and mechanical properties of sintered specimens were established according to the *P*–*h* dependencies obtained.

To determine Vickers hardness, to visualize indenter impressions, and to measure radial fracture lengths, a microhardness tester FALCON 500 (made by Innovatest, Maastricht, The Netherlands) equipped with a digital microscope and a five-megapixel matrix was used at 25 N load. To calculate microhardness and fracture toughness, a microhardness tester FALCON 500 was used with the licensed software IMPRESSIONS, which allowed for obtaining the values of mechanical characteristics in a semi-automated mode.

The flexural strength R_{bm} was determined using three-point flexural test with Instron 3344 universal testing machine (INSTRON Ltd., Norwood, MA, USA). During flexion, samples were registered by video at a rate of 10,000 frames per second, using a Photron FASTKA MMiniUX100 M1 high-speed video camera (Photron USA, Inc., San Diego, CA, USA). The compressive strength R_{cm} was evaluated using a Landmark MTS 870 Dual Column machine (made by MTS, Eden Prairie, MN, USA) at a displacement rate of 1 μm/s.

2.3. Initial Cutting Tests

In order to assess the effect of nano-VN addition on the wear resistance of the diamond composite cutting tools, initial cutting tests were performed. The segmented diamond cutting discs of diameter 320 mm for granite cutting were prepared and equipped with specially sintered segments. The cutting segments had a geometry of 40.0 mm × 12.0 mm × 3.2 mm and composition corresponding with samples 1, 5, and 6, i.e., with no VN addition, 2 wt.% and 4 wt.% of VN, respectively. AC160T diamond powder of 400/315 granularity, made by Diaprom OOO, (Kiev, Ukraine), in the amount of 1.54 carats per 1 cm^3 was added to the powder mixtures, which corresponded to the relative concentration of 35% in the respective powder mixtures. The initial cutting tests were performed in laboratory conditions.

3. Results and Discussion

3.1. Morphology of Initial Powders

The morphology of the applied iron, copper, nickel, and tin powders, as well as their mixtures, has been discussed in detail in [41]. It should be noted, that the surface of diamond bits had no defects like fractures or chipping. Iron powder particles had an average size of 25 μm and an irregular shape. Several larger iron particles, or rather agglomerates, were formed as a result of the coalescence of smaller particles. Copper powder particles sized 20 μm were less dense and exhibited a finer spatial dendritic structure with pronounced branches, which reduces the relative bulk density and prevents them from stacking compactly in a bulk state. Nickel powder particles with an average particle size of 15 μm were of a round shape with a very dense structure, which results, as in iron powders, in a high stacking density when in the bulk state. Tin powder particles averaging as big as 15 μm were spherical in shape, though particles with an elongated shape are encountered. There were metal overflows as well as small particles (satellites) on their surface. A round particle shape is well suited for their dense stacking in a bulk state. According to [38] research and ICPDS–ASTM datasheet [42], nano-VN powder particles demonstrated a three-phase structure: VN (cubic) with the crystal lattice period a = 0.4136 nm, $VN_{0,2}$, and VO_2 (hexagonal) with the crystal lattice period a = 0.4136 nm, b = 0.4517 nm, c = 0.5375 nm. The nano-VN powder particle size ranged from 0.1 to 0.7 μm with average ca. 0.5 μm). In the initial mixtures, a relatively uniform component distribution is observed, which is important for the subsequent sintering of composite samples.

3.2. Microstructure of Sintered CDM Samples

Figure 1 shows SEM images of typical areas of sintered samples, in the composite contrasting, illustrating features of the diamond–matrix interface. In sample 1, free of nano-VN additions, there are clearances up to 0.2 µm thick and discontinuities at the diamond–matrix interface, while voids are observable in the matrix away from the diamond–matrix interface (see Figure 1a,b). At the same time, in sample 5 containing nano-VN admixture, the diamond–matrix interface was tight without visible voids and discontinuities (see Figure 1c,d).

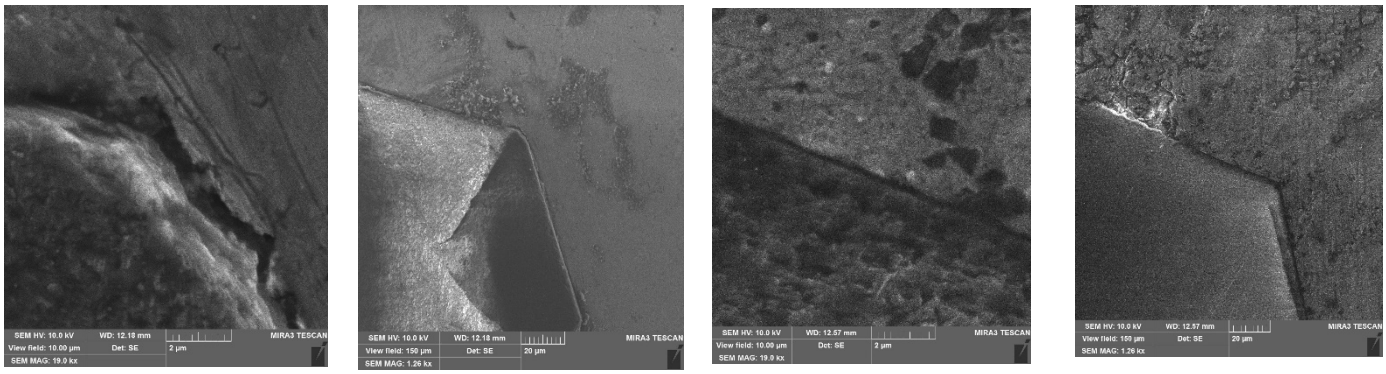

(**a**) (**b**) (**c**) (**d**)

Figure 1. SEM image of polished surface of diamond matrix samples based on 51Fe–32Cu–9Ni–8Sn matrices with different contents of nano-VN additive: (**a**,**b**) Sample 1 without VN addition; (**c**,**d**) Sample 5 with 2 wt.% of nano-VN.

It can be concluded that diamond bits in the samples with nano-VN addition adhered to the metal matrix stronger than those in samples without nano-VN. The adhesion mechanism of diamond grains to the metal matrix is not yet well investigated. Typically, the diamond–matrix interface is described by means of molecular, electrostatic, and chemical interactions, changes in the energy and structural states, and metal trapping. Most probably, the adhesion strength is conditioned by the simultaneous action of several of the aforementioned factors. However, the effect of each of them varies depending on the nature of the materials, their physical-mechanical and chemical properties, and on the parameters of the sintering process.

3.3. Effect of Nano-VN Additive on Mechanical Properties on Fe–Ni–Cu–Sn System

During the microhardness tests, the force F applied to an indenter is correlated with the depth h of its immersion to the material during the loading–unloading cycle. Figure 2 shows the respective plots obtained during nano-indentation for nano-VN inclusions in sintered samples 5, 6, 8, and 9, as well as for sample 1 with no nano-VN.

From Figure 1, a significant difference in the mechanical properties of the samples can be noted. At the equivalent indenter immersion depth in sample 5 surface, where 2 wt.% of nano-VN were added, the value of force applied to the indenter was two times greater than that for sample 1.

Higher values of force F for all samples with VN addition as compared to sample 1, indicate hardness increase due to the presence of nano-VN in the sample material. In general, an increase of nano-VN percentage in the tested composites caused an increase of force applied to the indenter. This phenomenon can be explained as follows. On the one hand, nano-VN particles are harder than 51Fe–32Cu–9Ni–8Sn, so that they have an effect on the hardness H and elastic modulus E of the composite. On the other hand, the inclusion of refractory nano-VN particles may act as barriers to dislocation propagation, which increases the composite strength. Table 2 presents the values of nanohardness H, elastic modulus E, elastic strain to failure expressed by H/E ratio, and resistance to plastic defor-

mation index H^3/E^2 for both 51Fe–32Cu–9Ni–8Sn sample 1 and samples 5, 6, 8, and 9 with nano-VN inclusions.

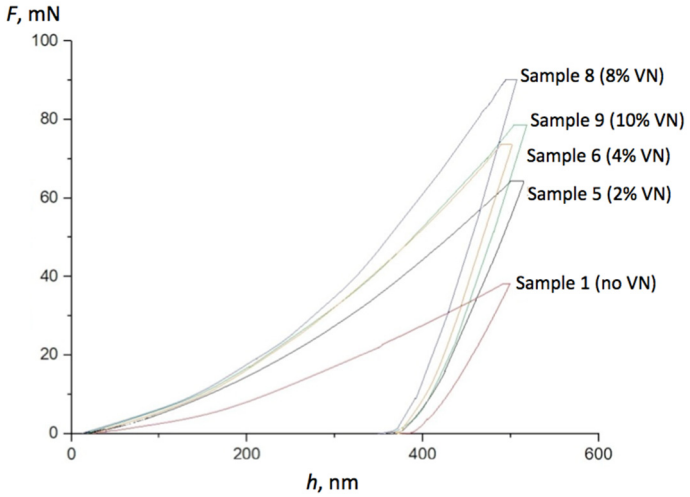

Figure 2. Plots of the force F versus the depth h during loading–unloading nano-indentation cycles for samples 1, 5, 6, 8, and 9, respectively.

Table 2. Mechanical characteristics of sintered matrix material 51Fe–32Cu–9Ni–8Sn and of nano-VN inclusions in it.

Sample No	H, GPa		E, GPa		H/E		H^3/E^2, MPa	
	Matrix	Inclusions	Matrix	Inclusions	Matrix	Inclusions	Matrix	Inclusions
1 (no VN)	5.2 ± 1.3	–	197 ± 11	–	0.0264	–	3.62	–
5 (2% VN)	5.6 ± 0.4	12.7 ± 0.3	202 ± 8	345 ± 12	0.0277	0.0368	4.30	17.21
6 (4% VN)	6.5 ± 0.6	14.8 ± 0.4	200 ± 8	390 ± 15	0.0325	0.0379	6.87	21.31
8 (8% VN)	7.8 ± 0.3	16.7 ± 1.7	213 ± 6	428 ± 31	0.0366	0.0390	10.46	25.42
9 (10% VN)	7.5 ± 0.6	14.8 ± 0.7	206 ± 16	388 ± 21	0.0364	0.0381	9.30	21.54

It is noteworthy that the matrix material itself increased all the parameters from $H = 5.2 \pm 1.3$ GPa, $E = 197 \pm 11$ GPa, $H/E = 0.0264$, and $H^3/E^2 = 3.62$ MPa for sample 1 and reaching maximal respective values for sample 8, namely, $H = 7.8 \pm 0.3$ GPa, $E = 213 \pm 6$ GPa, $H/E = 0.0366$, and $H^3/E^2 = 10.46$ MPa. The introduction of vanadium nitride nanopowder reinforcement into the composites apparently leads to an increase in the mechanical properties of the matrix itself. In fact, an increase of nano-VN content from 0 to 8 wt.% provided an increase of hardness H by 50%, modulus E by 8%, ratio H/E by 39%, and index H^3/E^2 even by 200% for the matrix material. Interestingly, the same parameters measured for the VN inclusions in the matrices of the respective samples, reached their maximal values for sample 8 with 8 wt.% of nano-VN.

The increase in hardness H and values H/E and H^3/E^2 at relatively low concentrations of vanadium nitride up to 8 wt.% in samples 5, 6, and 8 can be associated with a refinement of the matrix structure and reduction of void porosity, and also as a direct result of the nano-VN particles' presence due to their hardness and elastic modulus higher than that of iron, copper, nickel, and tin. However, the gradual decrease of H, E, H/E, and H^3/E^2 values in both matrix and inclusions of sample 9 with 10 wt.% of VN can be attributed to the agglomeration of nano-VN and the appearance of voids in them [38].

The values of microhardness H_v, fracture toughness K_{Ic}, flexural strength R_{bm} and compressive strength R_{cm} of sintered samples of 51Fe–32Cu–9Ni–8Sn material with different VN concentrations are listed in Table 3. The analysis of these results leads to the conclusion that with an increasing of VN concentration from 0 to 10% the microhardness H_v almost proportionally increased from 3.86 to 8.58 GPa, because of the significantly higher hardness

of VN than that of iron, copper, nickel, and tin. It is consistent with other researches which demonstrated that VN reinforcement promotes structure refinement [38] and increases the hardness and wear resistance of the composite [37].

Table 3. Mechanical characteristics of sintered samples with different VN content.

Sample No.	VN, wt.%	H_V, GPa	K_{Ic}, MPa·m$^{1/2}$	R_{bm}, MPa	R_{cm}, MPa
1	0	3.86	-	740	950
2	0.5	4.42	5.26	785	985
3	1.0	4.52	5.15	860	1098
4	1.5	4.91	5.12	992	1180
5	2.0	5.26	5.08	1071	1300
6	4.0	5.94	5.03	1110	1410
7	6.0	6.50	4.97	1078	1390
8	8.0	7.77	4.85	1012	1342
9	10.0	8.58	4.76	976	1313

In contrast, the addition of vanadium nitride in 51Fe–32Cu–9Ni–8Sn composite caused a slight decrease in the fracture toughness K_{Ic}. The absence of clear radial fractures in sample 1 shown in Figure 3a makes it impossible to determine the value of fracture toughness. The matrix material within the region surrounding the resultant indentation was almost intact and fractures were barely visible. At percentage 0.5 wt.% of VN, microindentation of sample 2 revealed the maximum value of fracture toughness K_{Ic} = 5.26 MPa·m$^{1/2}$. In this case, cracks appeared in the matrix around the indentation. Further increase in the nano-VN percentage in 51Fe–32Cu–9Ni–8Sn composite caused some, rather insignificant decrease in fracture toughness. Examples of the images of tested samples are shown in Figure 3b,c, corresponding with composited with 4 wt.% and 6 wt.% of VN, where radial cracks near the indentation are clearly seen. It can be noted that usually stiffness and fracture toughness exhibit opposite responses to structural changes in a material.

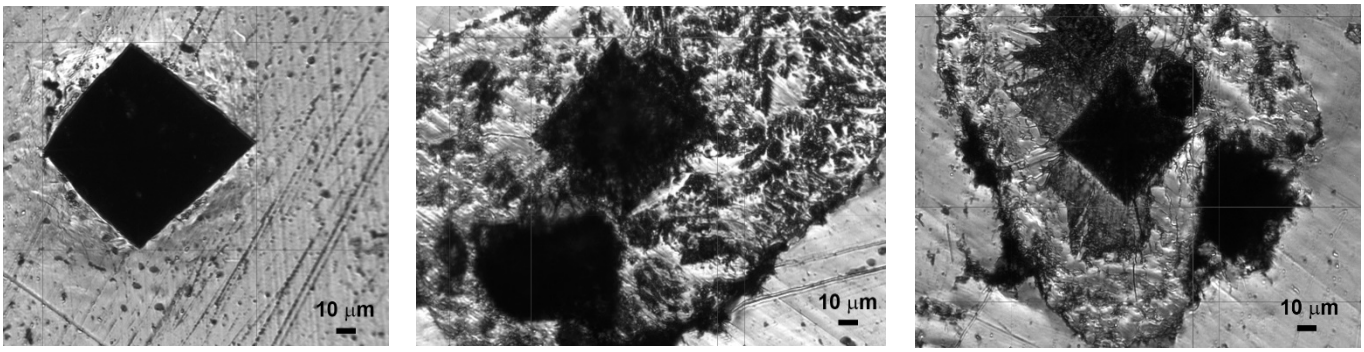

(**a**) (**b**) (**c**)

Figure 3. SEM images of indentations made in the surfaces of 51Fe–32Cu–9Ni–8Sn matrices with different contents of nano-VN additive: (**a**) Sample 1 without VN addition; (**b**) Sample 6 with 4 wt.% of nano-VN; (**c**) Sample 9 with 10 wt.% of nano-VN.

It was found that for sample 1 with no vanadium nitride reinforcement, the ultimate flexural strength was R_{bm} = 740 MPa, as specified in Table 3. When VN was added in a small amount of 0.5 wt.%, R_{bm} increased by 6% and increased further for higher concentrations of VN. However, it reached its maximum values R_{bm}= 1110 MPa for sample 6, which can be attributed to the grain structure refinement and a more even distribution of VN nanoparticles. The subsequent increase of VN concentration in samples 7–9 resulted in a gradual decrease of R_{bm} values, which perhaps was caused by the excessive embrittlement in the composite metal matrix promoted by the VN phase. Hence, the ultimate flexural strength R_{bm} reached its maximum for the composite with 4 wt.% of nano-VN reinforcement.

The positive effect of vanadium nitride addition to the composite has also been observed in the ultimate compressive strength R_{cm} presented in Table 3. Similarly, it reached its maximal value of R_{cm} = 1410 MPa in sample 6, where 4 wt.% of nano-VN reinforcement were present. Compared to sample 1, R_{cm} was improved by almost 50%, like ultimate flexural strength R_{bm}. Further increase in the VN concentration in the samples 7–9 slightly reduced the compressive strength, perhaps due to the gradually increasing embrittlement. Thus, general observation can be formulated that nano-VN reinforcement in the range from 0 up to 10% gradually increased microhardness and gradually decreased fracture toughness, but only at concentration 4 wt.% of VN ultimate compressive strength and ultimate flexural strength reached their maximal values.

The observed non-monotonic dependences of the studied composites' strength on VN content are the result of a complex combination of dispersion mechanism, strengthening and modification of their structures and phase compositions. It should be noted that the efficiency of the dispersion strengthening mechanism increases along with VN percentage, but the maximum values of fracture toughness, flexural and compressive strengths are attained in the samples with no VN additions. Such a change in the properties of sintered composites may correspond to a change in the phase composition after sintering and forming the final structure. Hence, the lack of direct proportionality between the structural changes and phase composition of sintered samples, as well as the effect of dispersion strengthening mechanism dependent on VN concentration, contributed to a non-linear effect of the content of VN reinforcement on H, K_{Ic}, R_{bm}, and R_{cm} values.

To sum up, it has been experimentally confirmed that the addition of nano-VN reinforcement to the Fe–Ni–Cu–Sn matrix is promising in terms of the fabrication of high-performance tools for the stonework industry. However, strict proportions of components should be observed, to avoid exceeding the threshold value of VN concentration and subsequent reduction in fracture toughness as well as in flexural and compressive strength.

3.4. Fractography and Failure Analysis

To assess failure resistance of the cutting tool composites, fracture analysis was found useful [43]. Figures 4 and 5 illustrate fracture patterns in samples 1 and 5, respectively, at various locations and magnifications.

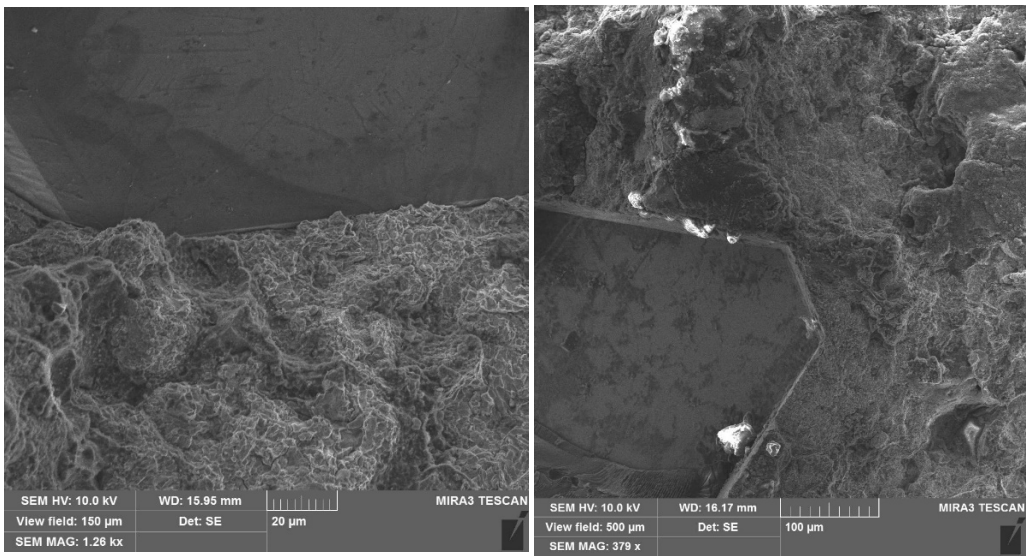

(**a**) (**b**)

Figure 4. Details of the fracture surface of diamond composite sample 1 at temperature +20 °C, adjacent to the diamond–matrix interface (**a**) 20 µm scale; (**b**) 100 µm scale.

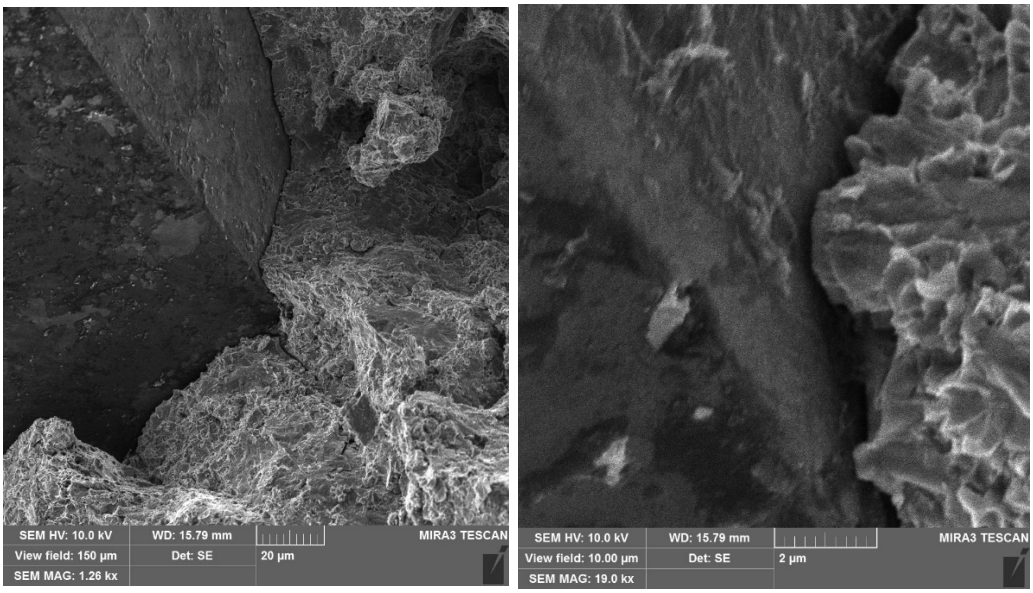

(**a**) (**b**)

Figure 5. Details of the fracture surface of diamond composite sample 5 at temperature +20 °C, adjacent to the diamond–matrix interface: (**a**) 20 µm scale; (**b**) 2 µm scale.

The samples underwent impact tests at 20 °C. In the fracture surface of sample 1 in Figure 4a,b, a viscous pitted relief prevails at micro- and macro levels as a result of cavities nucleation, their enlargement, and disruption of partitions between them. However, the matrix of sample 1 is dominated by equiaxed detachment-like pits, while the matrix of sample 5 revealed a structure more fine-grained and textured, as it can be seen in Figure 5a,b.

Furthermore, sample 1 (see Figure 4a,b) displays fewer pits, while in sample 5 (see Figure 5a,b) the number of pits increased. This suggests a positive effect of vanadium nitride addition on the mechanical properties of the diamond composite. An increase in the concentration of vanadium nitride in the tested samples did not result in qualitative changes in matrix fracture topography. However, it can be noted that the viscous growth area decreased and brittle through-grain damage accelerated. A specific feature of the obtained results is that the diamond grains surface in the samples with nano-VN additions shown in Figure 5a,b exhibited numerous inclusions in form of aggregates of irregular shape, as well as some metal residues. Such inclusions are distributed quite evenly across the diamond grain surface of sample 5, while no such inclusions were found on the diamond grain surface of sample 1.

Energy Dispersive Microanalysis (EDS) was carried out to determine the composition of phases developed during sintering. Figure 6 shows examples of SEM images of samples 1 and 5, obtained under the composite contrast, showing the areas where EDS microanalysis was performed. The results of elemental composition by weight ratio for these samples are collected in Table 4.

Based on the micro X-ray spectral analysis data it was revealed that sample 1 consisted of phases $C_{diamond}$ (spectra 1, 2, Table 4, Figure 6a), $C_{diamond}$, and C_{uB} in insignificant amounts (spectrum 3, Table 4, Figure 6a), FCC lattice of Cu-based solid solution and BCC of Fe-based solid solution with varied content of elements with a predominance of carbon, nickel, and copper (spectrum 4, Table 4, Figure 6a). The introduction of nano-VN in the amount of 2 wt.% into the composite sample 5 resulted in structure refinement. Sizes of the main components, in particular, iron and copper, were reduced (see Figure 6a,b respectively). In this case, the diamond–matrix interface became tight and free of visible clearances and gaps.

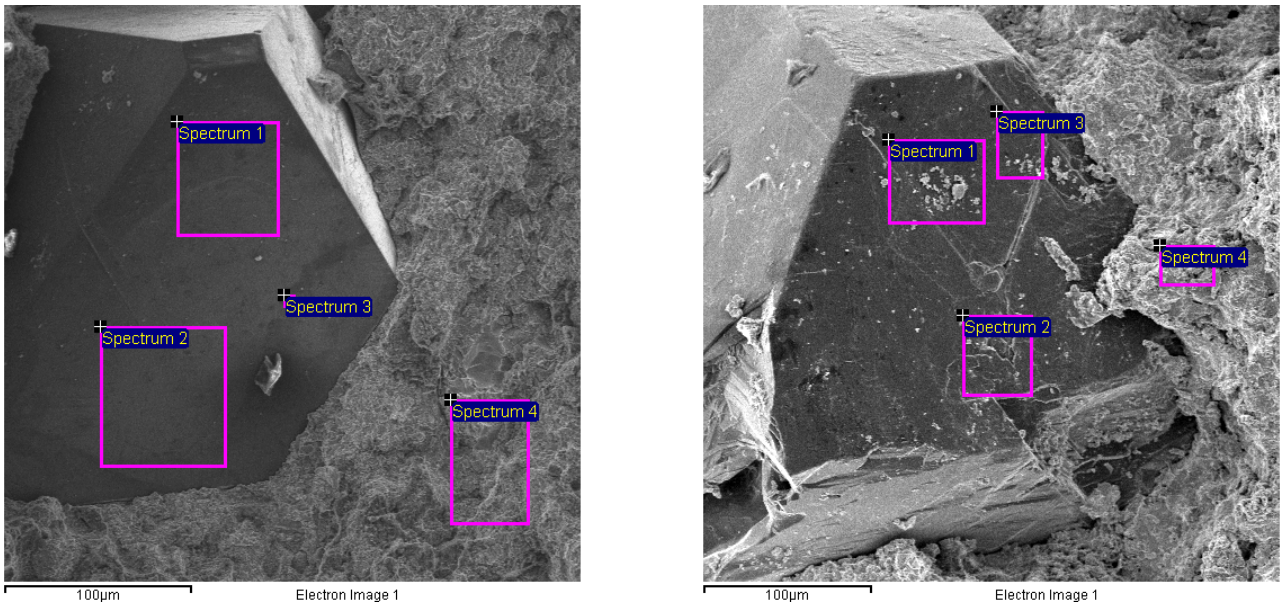

(**a**) (**b**)

Figure 6. SEM images of sintered samples microstructure, obtained under the composite contrast, showing EDS areas: (**a**) Sample 1; (**b**) Sample 5.

Table 4. Results of elemental analysis of different sections of samples 1 and 5, the spectra are specified in Figure 6.

Sample No	Spectrum	Percentage of Elements, wt.%						
		C	N	V	Fe	Ni	Cu	Sn
1	1	100.00	–	–	–	–	–	–
	2	100.00	–	–	–	–	–	–
	3	97.48	–	–	–	–	2.52	–
	4	12.72	–	–	68.62	9.00	8.73	0.92
5	1	89.99	–	2.39	4.71	1.52	1.39	–
	2	94.54	–	1.19	4.22	–	–	–
	3	90.16	–	2.50	6.51	–	0.83	–
	4	19.23	–	11.92	21.79	19.87	21.74	5.45

The structure of diamond composite sample 5 is made up of diamond grains ($C_{diamond}$) with small amounts of V, Fe, Ni, and Cu on their surfaces (spectra 1–3, Figure 6b, Table 4). FCC lattice of solid solutions containing iron, nickel, copper, vanadium, and tin in various combinations can be found, too (spectrum 4, Figure 6b, Table 4). This can be attributed to the fact that the addition of 2 wt.% of nano-VN improved the retention of diamond grains in the metal matrix and consequently increased the wear resistance of the composite.

It can be concluded that the addition of the required amount of nano-VN to the diamond composite based on the Fe–Cu–Ni–Sn matrix resulted in the dual effect of improving its mechanical properties. Namely, it ensured stronger chemical bonding between diamond grains and the metal matrix with simultaneous physical clamping of diamond grains in the metal composite matrix.

This, in turn, will allow efficient use of the diamond potential in the matrix that counteracts the diamond grains from being torn out of the metal matrix. Thereby, the increased wear resistance and productivity of tools are evident. In samples 6, 8, and 9, containing 4, 8, and 10 wt.% of nano-VN, respectively, the phase composition is similar to that of sample 5. The difference is only in the percentage of components in solid solutions.

The findings stay in agreement with those reported in [20,44], which indicated that the introduction of nano-VN to the tested Fe-Cu-based diamond composites improved their

mechanical properties, plasticity, and wear resistance, and attributed this to the dispersion strengthening and grain refinement caused by nano-VN. The authors noted that the gap width between a diamond grain and the matrix was from 3.99 to 2.06 µm in the composite with 2% of VN added. In [45] it was indicated that the mechanical properties of fine-grained diamond composite materials based on Fe–Cu matrix are higher than those of their coarse-grained counterparts. In the present researches, H and E values for sintered samples (see Table 2) significantly exceed H = 5.37 GPa and E = 125 GPa values of 51Fe–32Cu–9Ni–8Sn matrix material sample containing 3 wt.% of nano-VN reinforcement, formed under similar conditions [46]. Moreover, the hardness H = 5.2 GPa and elastic modulus E = 197 GPa, as well as the values of ration H/E = 0.0264 and index H^3/E^2 = 3.62 MPa of the sample 1 (see Table 2) significantly exceeded the previously reported values H = 2.68 GPa, E = 125 GPa, H/E = 0.013, and H^3/E^2 = 0.49 MPa of a similar sample sintered at temperature 800 °C with the subsequent hot post-pressing under the pressure of 160 MPa [36]. Moreover, it can be expected that a finely dispersed structure would increase the durability and cutting capability of the tools prepared using this method of hot-pressing [47–49].

3.5. Results of Initial Cutting Tests

The initial cutting tests were performed in laboratory conditions under the following cutting parameters:

- cutting depth for a single cut 0.10 m;
- longitudinal feeding speed 3 m/min;
- cutting speed 30 m/s;
- the coolant was the technical water of amounts 20 L/min;
- the volume of the cut granite corresponded with 10 m^2 of the cut surface.

The as-prepared cutting tools wear was assessed as linear material loss along the diameter of the disc. The initial results obtained under the abovementioned test conditions are summarized in Table 5 and in Figure 7.

Table 5. Results of initial cutting tests.

Tested Disc No	Composition of the Cutting Segments, wt.%	Linear Wear, mm
D1	8.75% $C_{diamond}$ + 46.5375% Fe + 29.2% Cu + 8.2175% Ni + 7.3% Sn	5.1 ± 0.058
D2	8.75% $C_{diamond}$ + 45.5175% Fe + 28.56% Cu + 8.0325% Ni + 7.14% Sn + 2% VN	3.4 ± 0.052
D3	8.75% $C_{diamond}$ + 44.4975% Fe + 27.92% Cu + 7.8525% Ni + 6.98% Sn +4% VN	2.5 ± 0.048

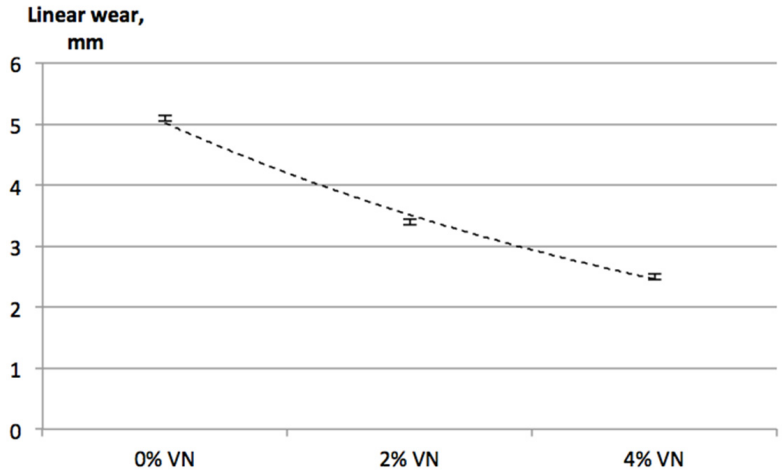

Figure 7. Linear wear of cutting discs with different additions of nano-VN.

From the initial test data collected in Table 5 and Figure 7, the overall trend marked with a dotted line is clearly seen. Linear wear along the disc diameter was 3.4 and 2.5 mm for the samples with additions of 2 wt.% and 4 wt.% nano-VN, respectively. Compared to the cutting tools sintered without VN additions, the wear decreased by 36% and 51%. Obviously, substantial improvement of the wear resistance observed in discs D2 and D3 was achieved through the mechanisms and phenomena described in previous sections, caused by VN addition to the composite of 8.75% $C_{diamond}$ + 46.5375% Fe + 29.2% Cu + 8.2175% Ni + 7.3% Sn powders. Strengthening of the metal matrix after VN was added is directly related to the increased nanohardness H, elastic deformation resistance H/E, and plastic deformation resistance H^3/E^2 specified in Table 2, as well as enhanced flexural strength R_{bm} and compressive strength R_{cm} specified in Table 3. In the case of the composite wear resistance improvement, an important role was played by the strengthened fixation of the diamond bits in the matrix, illustrated by the enhanced adhesion (see Figure 6).

These material investigations and initial cutting tests demonstrated significant potential economical benefits for the 8.75% $C_{diamond}$ + 46.5375% Fe + 29.2% Cu + 8.2175% Ni + 7.3% Sn composites with non-VN additions in two areas:

- energy and time-saving electroconsolidation technology used for samples fabrication;
- at least 30% increased lifetime of the diamond cutting discs when cutting hard, abrasive rocks.

Thereby, the use of nano-VN at concentrations 2, 4, 6, and 8 wt.% in a 51Fe–32Cu–9Ni–8Sn diamond composite matrix, and application of the vacuum hot pressing method within the temperature range of 20–1000 °C under the pressure of 30 MPa for 5 min was experimentally confirmed as a promising method for manufacturing of cutting tools with enhanced mechanical properties and high-performance feasible for the needs of stonework and mining industry. Potential economical benefits are obvious.

4. Conclusions

The fulfilled studies confirmed the positive effect of nano-VN reinforcement on the structure of the 51Fe–32Cu–9Ni–8Sn matrix and thus the mechanical properties of the diamond composites. In particular, nanohardness H, elastic modulus E, elastic deformation resistance H/E, plastic deformation resistance H^3/E^2, fracture toughness K_{Ic}, compressive strength R_{cm} and flexural strength R_{bm} were analyzed. The samples were first formed by cold-pressing, and then underwent a vacuum hot-pressing procedure. However, some of the properties worsened at various concentrations of the VN reinforcement. Some rules can be formulated as follows:

1. The diamond composites based on 51Fe–32Cu–9Ni–8Sn metal matrix with no VN reinforcement consisted of diamond grains and FCC of solid solutions containing iron, copper, nickel, and tin in different ratios. Some gaps and discontinuities were observed in the area of a diamond–matrix interface, and pores were found in the matrix.
2. Addition of nano-VN resulted in the formation of a finer-grained structure of the composites. They consisted of solid solutions incorporating iron, copper, nickel, vanadium, and tin in varying ratios. The formation of a tight diamond–matrix contact with no visible gaps, discontinuities, or other defects was observed. On the surface of diamond grains, metal overflows of Fe, Ni, V, Cu, and Sn were found.
3. Considering non-linear variations of the parameters, some sort of optimization can be considered in respect of nano-VN proportion. The maximum values of nanohardness H = 7.8 GPa, elastic modulus E = 213 GPa, ratio H/E = 0.0366, and index H^3/E^2 = 10.46 MPa were reached at proportion of 8 wt.% of nano-VN reinforcement, while maximal ultimate flexural strength R_{bm} = 1110 MPa and compressive strength R_{cm} = 1410 MPa were obtained at 4 wt.% of VN. At the same time, maximal fracture toughness corresponded with a minimal concentration of VN reinforcement. An excessive increase of nano-VN content in the tested composites demonstrated a decrease of mechanical properties due to the agglomeration of VN powder inclusions and the formation of gaps and discontinuities around them.

4. Initial cutting tests demonstrated improvement of wear resistance by 36% and 51%, which means substantially prolonged service time and effectiveness of the diamond cutting discs. Combined with the applied cheaper, less energy-consuming and time-saving electroconsolidation technology that allows for the achievement of the desired structures and properties, proposed composites appear economically very efficient.

It may be concluded that Fe–Cu–Ni–Sn–VN-based diamond composites exhibited enhanced physical and mechanical properties. Thus, they are feasible materials for the further development of cutting tools for various technological purposes. In the next stage of the research, as-prepared cutting tools will be tested in the terms of cutting parameters, performance, wear resistance during operation, and durability.

Author Contributions: Conceptualization, V.M. and N.B.; methodology, V.M. and A.M.; software, D.M. and W.S.; validation, B.R.; formal analysis, B.R., V.K. and D.M.; investigation, V.M., N.B. and V.K.; resources, W.S.; data curation, N.B.; writing—original draft preparation, V.K.; writing—review and editing, A.M., W.S. and D.M.; visualization, N.B. and W.S.; supervision, A.M.; project administration, V.M.; funding acquisition, V.M. and B.R. All authors have read and agreed to the published version of the manuscript.

Funding: This research was funded by Ministry of Education and Science of Ukraine, grant number 0120U100105. The works were supported also by the Scientific Committee of Ministry of Education and Science Republic of Kazakhstan.

Institutional Review Board Statement: Not applicable.

Informed Consent Statement: Not applicable.

Data Availability Statement: The data presented in this study are available on request.

Acknowledgments: The work was supported by Ministry of Education and Science of Ukraine, project registration number 0120U100105.

Conflicts of Interest: The authors declare no conflict of interest.

References

1. Morozow, D.; Barlak, M.; Werner, Z.; Pisarek, M.; Konarski, P.; Zagórski, J.; Rucki, M.; Chałko, L.; Łagodziński, M.; Narojczyk, J.; et al. Wear Resistance Improvement of Cemented Tungsten Carbide Deep-Hole Drills after Ion Implantation. *Materials* **2021**, *14*, 239. [CrossRef]
2. Li, M.; Sun, Y.; Meng, Q.; Wu, H.; Gao, K.; Liu, B. Fabrication of Fe-based diamond composites by pressureless infiltration. *Materials* **2016**, *9*, 1006. [CrossRef]
3. Zhao, X.; Duan, L. A review of the diamond retention capacity of metal bond matrices. *Metals* **2018**, *8*, 307. [CrossRef]
4. Borowiecka-Jamrozek, J.M.; Konstanty, J.; Lachowski, J. The application of aball-milled Fe–Cu–Ni powder mixture to fabricate sintered diamond tools. *Arch. Foundry Eng.* **2018**, *18*, 5–8.
5. Mariani, M.; Goncharov, I.; Mariani, D.; De Gaudenzi, G.P.; Popovich, A.; Lecis, N.; Vedani, M. Mechanical and microstructural characterization of WC–Co consolidated by binder jetting additive manufacturing. *Int. J. Refract. Met. Hard Mater.* **2021**, *100*, 105639. [CrossRef]
6. Hu, H.; Chen, W.; Deng, C.; Yang, J. Effect of matrix composition on the performance of Fe-based diamond bits for reinforced concrete structure drilling. *Int. J. Refract. Met. Hard Mater.* **2021**, *95*, 105419. [CrossRef]
7. Bulut, B.; Gunduz, O.; Baydogan, M.; Kayali, E.S. Determination of matrix composition for diamond cutting tools according to the hardness and abrasivity properties of rocks to be cut. *Int. J. Refract. Met. Hard Mater.* **2021**, *95*, 105466. [CrossRef]
8. Boland, J.N.; Li, X.S. Microstructural Characterisation and Wear Behaviour of Diamond Composite Materials. *Materials* **2010**, *3*, 1390–1419. [CrossRef]
9. Vynohradova, O.P.; Zakora, A.P.; Shul'zhenko, A.A.; Gargin, V.G.; Sokolov, A.N.; Efrosinin, D.V.; Zakora, I.A. Comparative Evaluation of the Performance of Drill Bits with a Diamond-Containing Matrix and Inserts Made of Diamond-Containing Composites. *J. Superhard Mater.* **2022**, *44*, 57–61. [CrossRef]
10. Huang, Y.; Zhang, F.; Zha, M.; Zhu, M.; Zhou, Y.; Tang, H.; Xie, D. Mechanical properties and tribological behavior of Fe/nano-diamond composite prepared by hot-press sintering. *Int. J. Refract. Met. Hard Mater.* **2021**, *95*, 105412. [CrossRef]
11. Dong, P.; Zhang, J.; Wu, J.; Wang, J. Performance investigation of traditional diamond frame saw in processing granite. *Int. J. Refract. Met. Hard Mater.* **2021**, *99*, 105601. [CrossRef]
12. Wang, S.; Zhang, J.; Dong, P. Comparison of wear characteristics of diamond segments under different sawing modes in sawing hard stone. *Int. J.Refract. Met. HardMater.* **2020**, *87*, 105149. [CrossRef]

13. Nitkiewicz, Z.; Swierzy, M. Tin influence on diamond-metal matrix hot pressed tools for stone cutting. *J. Mater. Proc. Tech.* **2006**, *175*, 306–315. [CrossRef]
14. Mechnik, V.A.; Bondarenko, N.A.; Kuzin, N.O.; Lyashenko, B.A. The role of structure formation in forming the physicomechanical properties of composites of the diamond–(Fe–Cu–Ni–Sn) system. *J. Frict. Wear.* **2016**, *37*, 377–384. [CrossRef]
15. Dinaharan, I.; Sathiskumar, R.; Murugan, N. Effect of ceramic particulate type on microstructure and properties of copper matrix composites synthesized by friction stir processing. *J. Mater. Res. Technol.* **2016**, *5*, 302–316. [CrossRef]
16. Dai, H.; Wang, L.; Zhang, J.; Liu, Y.; Wang, Y.; Wang, L.; Wa, X. Iron based partially pre-alloyed powders as matrix materials for diamond tools. *J. Powder Metall.* **2015**, *58*, 83–86. [CrossRef]
17. Wang, J.; Han, Y.; Zhao, Y.; Li, X.; Yi, D.; Guo, Z.; Cao, Y.; Liu, B.; Tang, H.P. Microstructure and properties of WC-12Co cemented carbide fabricated via selective electron beam melting. *Int. J. Refract. Met. Hard Mater.* **2022**, *106*, 105847. [CrossRef]
18. Kolodnits'kyi, V.N.; Bagirov, O.E. On the structure formation of diamond containing composites used in drilling and stone working tools (A review). *J. Superhard Mater.* **2017**, *39*, 1–17. [CrossRef]
19. Mechnik, V.A.; Bondarenko, N.A.; Kuzin, N.O.; Gevorkian, E.S. Influence of the addition of vanadium nitride on the structure and specifications of a diamond–(Fe–Cu–Ni–Sn) composite system. *J. Frict. Wear.* **2018**, *39*, 108–113. [CrossRef]
20. Han, Y.; Zhang, S.; Bai, R.; Zhou, H.; Su, Z.; Wu, J.; Wang, J. Effect of nano-vanadium nitride on microstructure and properties of sintered Fe–Cu-based diamond composites. *Int. J. Refract. Met. Hard Mater.* **2020**, *91*, 105256. [CrossRef]
21. Cygan-Bączek, E.; Wyżga, P.; Cygan, S.; Bała, P.; Romański, A. Improvement in Hardness and Wear Behaviour of Iron-Based Mn–Cu–Sn Matrix for Sintered Diamond Tools by Dispersion Strengthening. *Materials* **2021**, *14*, 1774. [CrossRef]
22. Mechnik, V.A. Production of diamond–(Fe–Cu–Ni–Sn) composites with high wear resistance. *Powder Metall. Met. Ceram.* **2014**, *52*, 577–587. [CrossRef]
23. Leyland, A.; Matthews, A. On the significance of the H/E ratio in wear control: A nanocomposite coating approach to optimized tribological behaviour. *Wear* **2000**, *246*, 1–11. [CrossRef]
24. Musil, J. Tribological and mechanical properties of nanocrystalline n-TiC/a-C nanocomposite thin films. *J. Vac. Sci. Technol. A.* **2010**, *28*, 244–249. [CrossRef]
25. Gevorkyan, E.; Mechnik, V.; Bondarenko, N.; Vovk, R.; Lytovchenko, S.; Chishkala, V.; Melnik, O. Peculiarities of obtaining diamond–(Fe–Cu–Ni–Sn) hot pressing. *Funct. Mater.* **2017**, *24*, 31–45. [CrossRef]
26. Uemura, M. An Analysis of the catalysis of Fe, Ni, or Co on the wear of diamonds. *Tribol. Int.* **2004**, *37*, 887–892. [CrossRef]
27. Bondarenko, M.O.; Mechnik, V.A.; Suprun, M.V. Shrinkage and shrinkage rate behavior in Cdiamond–Fe–Cu–Ni–Sn–CrB_2 system during hot pressing of pressureless-sintered compacts. *J. Superhard Mater.* **2009**, *31*, 232–240. [CrossRef]
28. de Oliveira, L.J.; Bobrovnitchii, G.S.; Filgueira, M. Processing and characterization of impregnated diamond cutting tools using a ferrous metal matrix. *Int. J. Refract. Met. Hard Mater.* **2007**, *25*, 328–335. [CrossRef]
29. Borowiecka-Jamrozek, J.; Lachowski, J. Modelling of the mechanical state of a diamond particle in the metallic matrix. *Adv. Mater. Res.* **2014**, *874*, 127–132. [CrossRef]
30. Oliveira, F.A.C.; Anjinho, C.A.; Coelho, A.; Amaral, P.M.; Coelho, M. PM materials selection: The key for improved performance of diamond tools. *Met. Powder Rep.* **2017**, *72*, 339–344. [CrossRef]
31. Wang, J.; Shang, S.; Peng, F. Influence mechanism of hard brittle grits on the drilling performance of diamond bit. *Ann. Chim.-Sci. Matériaux* **2018**, *42*, 209–220. [CrossRef]
32. Wu, Y.; Yan, Q.; Zhang, X. Wear characteristics of Fe-based diamond composites with cerium oxide (CeO_2) reinforcements. *Int. J. Refract. Met. Hard Mater.* **2020**, *86*, 105093. [CrossRef]
33. Mechnyk, V.A. Regularities of structure formation in diamond–Fe–Cu–Ni–Sn–CrB_2 systems. *Mater. Sci.* **2013**, *49*, 93–101. [CrossRef]
34. Mechnik, V.A. Effect of hot recompaction parameters on the structure and properties of diamond–(Fe–Cu–Ni–Sn–CrB_2) composites. *Powder Metall. Met. Ceram.* **2014**, *52*, 709–721. [CrossRef]
35. Mechnik, V.A.; Bondarenko, N.A.; Kolodnitskyi, V.M.; Zakiev, V.I.; Zakiev, I.M.; Ignatovich, S.R.; Yutskevych, S.S. Mechanical and tribological properties of Fe−Cu−Ni−Sn materials with different amountsof CrB_2 used as matrices for diamond-containing composites. *J. Superhard Mater.* **2020**, *42*, 251–263. [CrossRef]
36. Mechnik, V.A.; Bondarenko, N.A.; Kolodnitskyi, V.M.; Zakiev, V.I.; Zakiev, I.M.; Ignatovich, S.R.; Dub, S.N.; Kuzin, N.O. Effect of vacuum hot pressing temperature on the mechanical and tribological properties of the Fe–Cu–Ni–Sn–VN composites. *Powder Metall. Met. Ceram.* **2020**, *58*, 679–691. [CrossRef]
37. Mechnik, V.A.; Bondarenko, N.A.; Kolodnitskyi, V.M.; Zakiev, V.I.; Zakiev, I.M.; Storchak, M.; Dub, S.N.; Kuzin, N.O. Physico-mechanical and tribological properties of Fe–Cu−Ni−Sn and Fe−Cu–Ni−Sn–VN nanocomposites obtained by powder metallurgy methods. *Tribol. Ind.* **2019**, *41*, 188–198. [CrossRef]
38. Mechnik, V.A.; Bondarenko, N.A.; Dub, S.N.; Kolodnitskyi, V.M.; Nesterenko, Y.V.; Kuzin, N.O.; Zakiev, I.M.; Gevorkyan, E.S. A study of microstructure of Fe–Cu–Ni–Sn and Fe–Cu–Ni–Sn—-VN metal matrix for diamond containing composites. *Mater. Charact.* **2018**, *146*, 209–216. [CrossRef]
39. Gevorkyan, E.; Lavrynenko, S.; Rucki, M.; Siemiątkowski, Z.; Kislitsa, M. Preparation of nanostructured materials by electrical sintering. In Proceedings of the 7th International Conference on Mechanics and Materials in Design (M2D2017), Albufeira, Portugal, 11–15 June 2017; Silva Gomes, J.F., Meguid, S.A., Eds.; INEGI: Porto, Portugal, 2017; pp. 663–666.

40. Oliver, W.C.; Pharr, G.M. An improved for determining hardness and elastic modulus using load and displacement sensing indentation experiments. *J. Mater. Res.* **1992**, *7*, 1564–1583. [CrossRef]
41. Mechnik, V.A.; Bondarenko, N.A.; Kolodnitskyi, V.M.; Zakiev, V.I.; Zakiev, I.M.; Kuzin, M.O.; Gevorkyan, E.S. Influence of diamond–matrix transition zone structure on mechanical properties and wear of sintered diamond-containing composites based on Fe–Cu–Ni–Sn matrix with varying CrB_2 content. *Int. J. Refract. Met. Hard Mater.* **2021**, *100*, 105655. [CrossRef]
42. *Selected Powder Diffraction Data for Education Straining (Search Manual and Data Cards)*; International Centre for Diffraction Data: Swarthmore, PA, USA, 1988.
43. Gevorkyan, E.; Rucki, M.; Panchenko, S.; Sofronov, D.; Chałko, L.; Mazur, T. Effect of SiC Addition to Al_2O_3 Ceramics Used in Cutting Tools. *Materials* **2020**, *13*, 5195. [CrossRef] [PubMed]
44. Mechnik, V.; Bondarenko, N.; Kolodnitskyi, V.; Zakiev, V.I.; Zakiev, I.M.; Gevorkyan, E.S.; Kuzin, N.O. Microstructural Features and Mechanical and Tribological Properties of Fe–Cu–Ni–Sn Composites Precipitation-Hardened with CrB_2 Additions. *Powder Metall. Met. Ceram.* **2021**, *60*, 204–215. [CrossRef]
45. He, L.; Ma, E. Processing and microhardness of bulk Cu–Fe. *Nanostruct. Mater.* **1996**, *7*, 327–339. [CrossRef]
46. Mechnik, V.A.; Bondarenko, N.A.; Kolodnitskyi, V.M.; Zakiev, V.I.; Zakiev, I.M.; Ignatovich, S.R.; Dub, S.N.; Kuzin, N.O. Formation of Fe-Cu-Ni-Sn-VN nanocrystalline matrix by vacuum hot pressing for diamond-containing composite. Mechanical and Tribological Properties. *J. Superhard Mater.* **2019**, *41*, 388–401. [CrossRef]
47. Gevorkyan, E.; Prikhna, T.; Vovk, R.; Rucki, M.; Siemiatkowski, Z.; Kucharczyk, W.; Chishkala, V.; Chałko, L. Sintered nanocomposites ZrO_2-WC obtained with field assisted hot pressing. *Compos. Struct.* **2021**, *259*, 113443. [CrossRef]
48. Chishkala, V.; Lytovchenko, S.; Mazilin, B.; Gevorkyan, E.; Shkuropatenko, V.; Voyevodin, V.; Rucki, M.; Siemiątkowski, Z.; Matijošius, J.; Dudziak, A.; et al. Novel Microwave-Assisted Method of $Y_2Ti_2O_7$ Powder Synthesis. *Materials* **2020**, *13*, 5621. [CrossRef]
49. Gevorkyan, E.; Rucki, M.; Sałaciński, T.; Siemiątkowski, Z.; Nerubatskyi, V.; Kucharczyk, W.; Chrzanowski, J.; Gutsalenko, Y.; Nejman, M. Feasibility of Cobalt-Free Nanostructured WC Cutting Inserts for Machining of a TiC/Fe Composite. *Materials* **2021**, *14*, 3432. [CrossRef]